Journal of Electron Devices, Vol. 20, 2014, pp. 1733-1739

JED [ISSN: 1682 -3427]

Journal of Electron Devices
www.jeldev.org

ELECTRICAL CONDUCTION MECHANISM IN THE HIGH TEMPERATURES FOR THIN-FILM TRANSISTOR UTILIZING TUNNEL EFFECT.

Takahiro Kobayashi, Naoto Matsuo, Yasuhisa Omura[1], Shin Yokoyama[2], Akira Heya
Department of Materials Sciences and Chemistry, University of Hyogo
[1]Graduate School of Science and Engineering, Kansai University
[2]Department of Semiconductor Electronics and Integration Sciences, Hiroshima University
ew10k502@steng.u-hyogo.ac.jp

Received 7-07-2014, online 14-07-2014

Abstract

The Tunneling-Dielectric TFT (TDTFT), that has thin dielectric films at both ends of the channel fabrication area, was fabricated with 1.7 nm SiN_X film by LPCVD method. The conduction mechanism of the drain currents was examined in the temperatures from 293 to 623 K experimentally and theoretically. The I_d-V_g characteristics were reproduced by the direct tunneling (DT) via SiN_X film with an assumption of the electron effective mass of 0.25 corresponding to the one-band model. The DT from the tail of the Fermi-Dirac distribution of Al electrode to n^+ doping area of poly-Si influences greatly on the drain currents.

Keyword: Tunneling-Dielectric TFT, SiN_X, Direct tunneling, High temperature.

I. INTRODUCTION

Recently, thin-film transistor (TFT) is used for pixel of organic electro luminescence display (OEL) [1] as well as liquid crystal display (LCD) [2]. However, the drain current at the off-state voltage is large for the conventional TFT. It is important to decrease the off-state current of the TFTs to realize a high speed, a high brightness and a low power consumption for the performance of the display [3, 4]. We proposed the tunneling dielectric TFT (TDTFT) that has very thin dielectric film at both ends of channel for the improvement of channel leakage current [5, 6]. The TDTFT is the device similar to the tunneling MOS transistor (TMOST) [7] which was presented for the fine MOSFET. The important point of the configuration of the TMOST is that it has the very thin dielectric film between the source/drain and the channel, and the performance of the TMOST is dominated by the tunnel emission from the source to the channel. The TDTFT controls the number of the electrons in the channel by the direct tunneling (DT) through the thin dielectric film as well as the TMOST. The off-state current of the TDTFT decreased to approximately 1/10 in comparison with a conventional TFT by using a very thin silicon nitride film (SiN_X) as tunneling dielectric film [8]. Furthermore, we reported that the dominant conduction mechanism of TDTFT at low temperatures ranging from 20 K to 150 K is the DT through the thin dielectric film [9].

By the way, the tunnel FET (TFET) which utilizes the band-to-band tunneling (BTBT) mechanism has been researched and developed intensively [10-14]. The improvements of the on-state current and off-state current of the TFET are the crucial issues, and therefore the examinations related to the materials such as SiGe or Ge and the device structure such as a double-gate architecture has been pursuit. The operation principle of the TFET is the tunnel emission from the source to the channel via energy band-gap.

The novelty of the present research is as follows. We presented the TDTFT to increase the dynamic range of the drain currents between the on-state and off-state for the gate. Therefore, the examination of the operation principle of the TDTFT is very crucial. In this paper, we examine the conduction mechanism of the TDTFT, that has SiN_X film as tunneling dielectric film, at high temperatures ranging from 293 K to 623 K theoretically and experimentally.

II. EXPERIMENT

II.1. Experimental method

Fig. 1 shows the cross section view of the bottom-gate TDTFT. The thickness of SiN_x was 1.7 nm. It was fabricated between the Aluminum (Al) layer and n^+ doping layer that serves as the source and drain electrodes. The 2-inch n^+ Si

(100) wafer was doped by antimony (Sb) and has a resistivity of 0.007 to 0.02 Ohm-cm. The wafer was utilized as

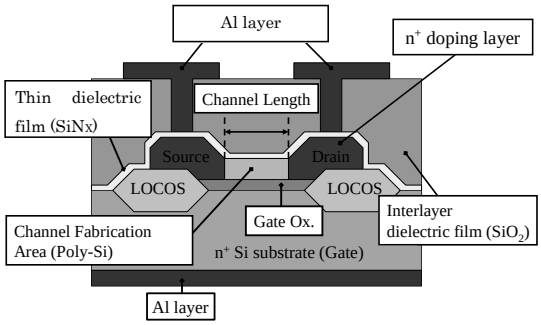

Fig. 1: Cross section view of bottom-gate TDTFT.

the gate electrode, and processed, as follows. The field oxide and the gate oxide with thicknesses of 280 nm and 66.4 nm were formed in turn by the local oxidation of silicon (LOCOS) method at 1000 ℃ for 3 h and by the dry oxidation at 850 ℃ for 50 min, respectively. The poly-Si which serves as the channel was deposited by low-pressure CVD (LPCVD) at 635 ℃. The source and drain regions were formed by the ion implantation (i. i.) of arsenic (As) at 10 KeV with a concentration of 1×10^{15} cm^{-2}. After the i. i., the wafer was annealed at 850 ℃ for 10 min in oxygen atmosphere for the activation of the As. Then, the oxide film was removed by HF aqueous solution. The tunneling SiN_X dielectric film was deposited by LPCVD at 750 ℃ for 3 min. The SiO_2 passivation layer was deposited by atmospheric-pressure CVD (APCVD). Then, the contact hole was formed by the wet etching. Al layer was formed by the sputtering method. Thickness of Al layers of the front and back sides are 800 and 400 nm, respectively. Hydrogen annealing at 400 ℃ for 30 min was performed. The conventional TFT was fabricated by the same processes as the TDTFT. But, the tunneling dielectric film was not deposited on the conventional TFT. The film thickness was measured using a spectroscopic ellipsometer (J. A. Woollam, Japan Co., Inc.), and the uniformity of SiN_X film was measured using a transmission electron microscopy (TEM).

The I_d-V_g characteristics were measured at temperatures from 293 K to 623 K. This temperature range is denoted as high-temperature condition. The channel length L and the channel width W of conventional TFT and TDTFT are 10 μm and 50 μm, respectively.

II.2. Calculation method

The tunnel current is given by the eq.(1) [15, 16]

$$J_{nt} = \frac{4\pi m^* e}{h^3}\int_{E_{fm2}}^{E_{max}}\left[\int_0^{\infty} (f_m - f_s)\,dE_t\right]\times \exp\left[-\gamma_n(\bar{\psi}_m - E_{fm1} - E_x)^{1/2}\right] dE_x \qquad (1)$$

where, J_{nt}, e, h, m^*, E_X, E_t, E_{fm1}, E_{fm2}, f_m, f_S, and $\bar{\psi}_m$ are the total tunnel current, the electric charge, Planck's constant, the effective mass of electron, the energy component of the incident electron in the X direction, the energy component of the incident electron normal to the X direction, the Fermi-energy of Al and that of poly-Si, the Fermi-Dirac distribution function (FD function) of Al and that of poly-Si, and the average energy height of the tunnel barrier, respectively. In the present experiment, the electrons are emitted from Al electrode to poly-Si via SiN_x film by the DT.

Fig.2 shows the Fermi-energy surface of k-space by which the electron distribution contributing to the DT is shown, E_f, eV, k_B, k_x, $k_\perp$ and T are the Fermi-energy of the Al at the emission side, the applied voltage, Boltzman constant, the wave number of the incident electron in the X direction and that normal to the X direction and the absolute temperature.

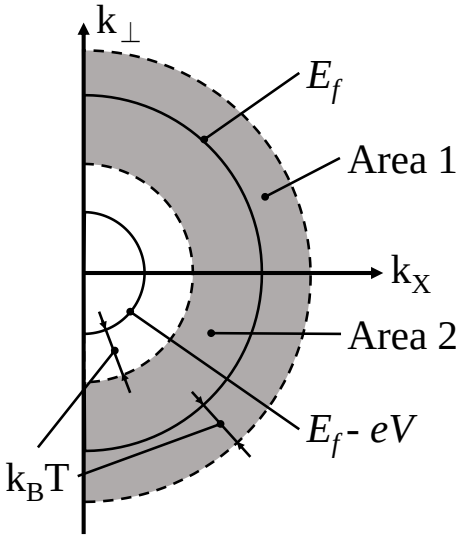

Fig. 2: The Fermi energy surface for k-space.

The outer solid line denoted by E_f is the Fermi-surface of the Al at the emission side and the inner solid line denoted by (E_f -eV) is the Fermi-surface of the poly-Si at the incident side. The Fermi-energy surface is spread by k_BT, and therefore the electron distribution which contributes to the DT is shown by the dark areas

denoted by area 1 and area 2. By considering the temperature, the total DT currents are divided to the component J_{nt1} which corresponds to the area 1 larger than the Fermi-energy of Al and the component J_{nt2} which corresponds to the area 2 smaller than the Fermi-energy of Al. The total DT currents are obtained by eq.(2).

$$J_{nt} = J_{nt1} + J_{nt2} \quad . \tag{2}$$

By assuming the total electron energy as E_f+k_BT in the area 1, the interval of E_X and E_t are E_f~E_f+k_BT and 0~$E_f+k_BT-E_X$, respectively. Here, the upper limit is replaced by ∞ for simplification of the integral calculation. In addition, assuming the total electron energy as E_f in the area 2, the interval of E_X and E_t are E_f-eV+k_BT~E_f and 0~E_f-E_X, respectively [17, 18].

Here, the actual band diagram is shown to calculate the J_{nt1} and J_{nt2}. Figs. 3 (a) and (b) show the actual band diagrams of the TDTFT before and after application of the gate voltage in the high temperatures. For the Al layer and n^+ doping layer, the relationships between the electron density and the electron energy are shown. J_{nt1} and J_{nt2} are given by integrating eq. (1) as follows.

In eq. (1), J_{nt1} has $f_m = \exp[-\beta(E_t + E_x - E_{fm1})]$ and $f_S = \exp[-\beta(E_t + E_x - E_{fm2})]$. Here, E_t and E_X are integrated by 0 to ∞ and E_{fm1} to ∞ in the integral range, respectively. The J_{nt1} was given by the following eq. (3):

$$J_{nt1} = 4\pi m^* e(k_B T)^2/h^3 \times \left[-\gamma_n/2\beta\bar{\psi}_m^{1/2}\right]^{-1} \times \exp(-\gamma_n\bar{\psi}_m^{1/2}) \times (1-\exp(\beta V_{app})) \tag{3}$$

where $\gamma_n = 4\pi(2m^*)^{1/2} t_{SiN}/h$.

In eq. (1), J_{nt2} has $f_m = 1$ and $f_S = \exp[-\beta(E_t + E_x - E_{fm2})]$. Here, E_t and E_X are integrated by 0 to E_{fm1}-E_X and E_{fm2} to E_{fm1} in the integral range, respectively. The J_{nt2} was given by the following eq. (4):

$$J_{nt2} = \frac{4\pi m^* e}{h^3} \times \frac{2(E_{fm1}-E_{fm2})\bar{\psi}_m^{1/2}}{3\gamma_n} \times \exp(-\gamma_n\bar{\psi}_m^{1/2}) - \frac{4\pi m^* e}{h^3} \times \frac{2(E_{fm1}-E_{fm2})(\bar{\psi}_m + E_{fm1} - E_{fm2})^{1/2}}{3\gamma_n} \times \exp\left[-\gamma_n(\bar{\psi}_m + E_{fm1} - E_{fm2})^{1/2}\right] \tag{4}$$

t_{SiN} is the thickness of SiN_X film. β and qV_{app} are shown by $(k_BT)^{-1}$ and E_{fm1}-E_{fm2}, respectively.

The applied voltage to the tunneling dielectric film is calculated by eq. (5):

$$V_{tun} = R_{tun} \times I_{TD} \tag{5}$$

with, $$R_{tun} = \frac{1}{2}\left(\frac{V_d}{I_{TD}} - \frac{V_d}{I_{Co}}\right). \tag{6}$$

where, R_{tun}, I_{TD}, I_{Co}, V_d and V_{tun} are the resistance of tunneling dielectric film, drain current of TDTFT, drain current of conventional TFT, drain voltage and applied voltage to the tunneling dielectric film, respectively. When the drain voltage is 2.5 V, the applied voltage to the tunneling dielectric film at 293 K and 353 K are 8.0×10^{-2} V and 9.8×10^{-2} V, respectively. The total drain current of TDTFT was calculated by the multiplication of J_{nt} and tunneling probability of the tunneling dielectric film at the drain side.

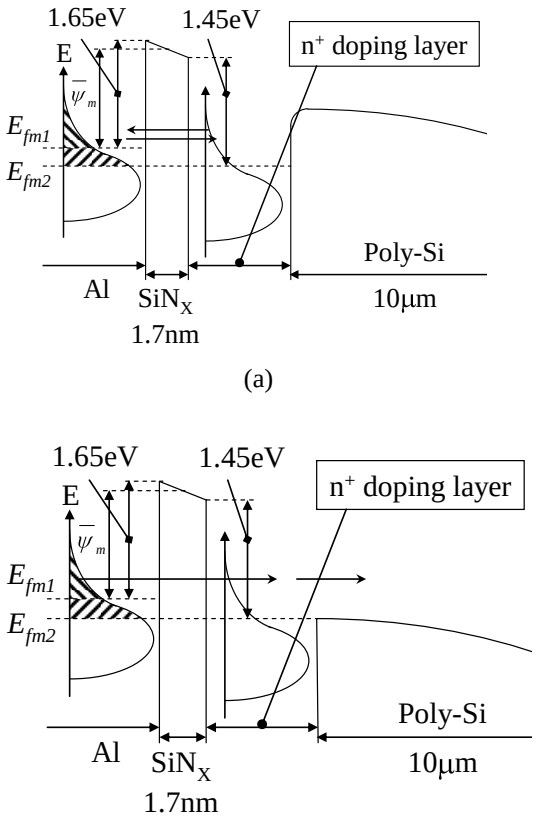

Fig. 3: Band diagram of TDTFT at a high temperature without (a) and with (b) application of bias voltage.

The energy barrier between the doping layer and poly-Si is formed as shown in Fig.. 3 (a), because

the channel is not formed before the gate voltage application. At the drain voltage application, the electron is emitted from Al layer to the n^+ doping layer by DT via SiN_X film, and the electron is reflected by energy barrier. However, at the gate voltage application, the electron is emitted from Al layer to the channel by DT via SiN_X film as shown in Fig. 3 (b), because the energy barrier disappears by the gate voltage application.

III. RESULTS AND DISCUSSION

Figures.4 (a) and (b) show the I_d-V_g characteristics of the TDTFT and conventional TFT. The slope of the subthreshold region of the TDTFT is smaller than that of the conventional TFT. This phenomenon is due to the tunnel resistivity of the SiN_X film formed at the source/drain area of the TDTFT. Although the leakage currents of the TDTFT and the conventional TFT are almost the same, the off-state voltage of the TDTFT is a little larger than that of the conventional TFT. This is thought to be due to the difference of the Fermi-level for poly-Si served as the active layer between the TDTFT and conventional TFT. As the Fermi-level of the TDTFT is lower than that of the conventional TFT, the leakage current at the Vg=0 V of the TDTFT increases. Therefore, the leakage current of the TDTFT is smaller than that of the conventional TFT by using the poly-Si with an identified Fermi level [8]. Here, the origin of the carriers in the subthreshold region generated by increasing the temperatures is discussed. The carriers are excited from the defect level equal to 0.15eV [9] from the band edge for T=293~453K and excited from the valence band for the temperatures larger than 623K in the intrinsic semiconductor region. The conduction of the excited carriers in the channel is dominated by the tunnel emission via SiNx film at the source/drain side as discussed later. It is finally confirmed that the TDTFT shows the characteristic peculiar to the tunnel effect of the SiN_X film and it improves the conventional TFT. Next, we analyzed the conduction of the TDTFT in the high temperature using eq. (2).

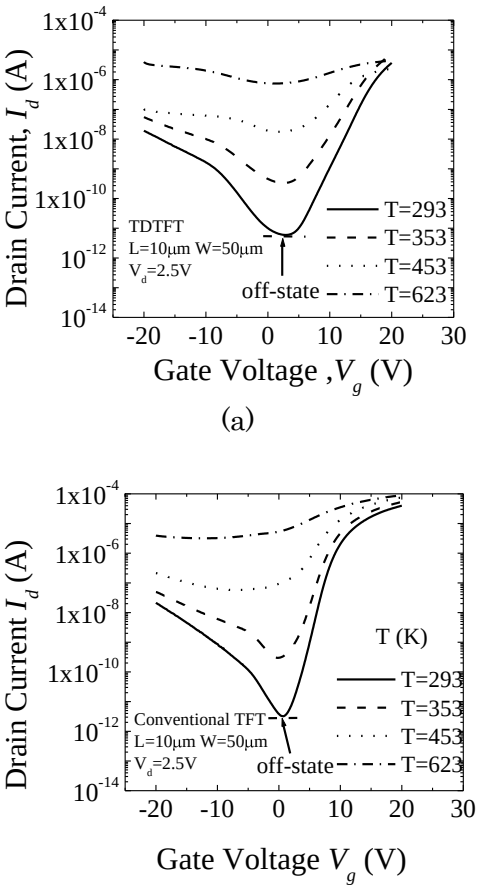

Fig. 4: The I_d-V_g characteristics of the TDTFT (a) and conventional TFT (b).

Fig. 5 shows the relationship between calculated and measured drain currents of the TDTFT. The inset is an enlarged view around the threshold voltage in Fig. 4 for the temperatures of 293 K and 353 K. The threshold voltage for each temperature was decided by the interpolation of I_d-V_g curve. The drain current was identified at the threshold voltage for each temperature. The conditions for the DT current simulation are as follows. The thickness of SiN_X film and effective mass are t_{SiN} = 1.3 nm and m^*/m_0 = 0.25, respectively. When the temperature increases from 293 K to 353 K, the conduction band edge of Si is decreased by 0.02 eV, because of a band gap decrease with temperature [19]. The band gap of SiN_X film is 4.4 eV [20]. At 293 K, the calculated value of DT current is 7.4×10^{-7} A that is nearly equal to the measured value of 7.5×10^{-7} A. And, at 353 K, it is 1.1×10^{-6} A that is nearly equal to the measured value of 1.2×10^{-6} A. Furthermore, the limit of temperature that dominates the DT exists between 350 K and 400 K from the calculated result. In addition, the J_{nt1} at

293 K and 353 K are 1.3×10^{-7} A and 2.1×10^{-7} A, respectively, and J_{nt2} at 293 and 353 K are 6.1×10^{-7} A and 8.5×10^{-7} A, respectively. These data strongly indicate that the dominant conduction mechanism of the TDTFT is the DT. The tail area of the FD function larger than the Al Fermi energy influences greatly on the DT. Although the thickness of SiN_X film was assumed to be 1.3 nm, it is thought that the thickness is within the measurement error of spectroscopic ellipsometer. The effective mass was calculated by the extrapolation of the calculated effective mass as a function of the oxide thickness [21]. As a result, the effective mass of SiN_X film was given to be 0.25 in the present experiment. In the case of thick film of a few nm, the effective mass of 0.42 is used in the two-band model [22,23]. But, in the case of thin film, the effective mass decreases to 0.33±0.08 corresponding to one-band model [24]. In the present calculation, the effective mass at one-band model was used, because of the thickness for SiN_X film being small.

The drain current is uncontrollable in the gate voltage application for the higher temperature greater than or equal to 453 K considering Fig. 4 and Fig. 5. The reason of this phenomenon is as follows. The change of the electron carrier concentration in the channel by the gate voltage application is small, because many electron carriers are already generated for non-gate application in the high temperatures. Thus, it is concluded that the conduction mechanism is the DT from 293 K to 353 K and the tail area of the FD function larger than the Fermi energy of Al greatly influences the conduction mechanism of the TDTFT. The DT from 293 K to 353 K for the TDTFT is different from that in the low temperatures from 20 K to 150 K [9].

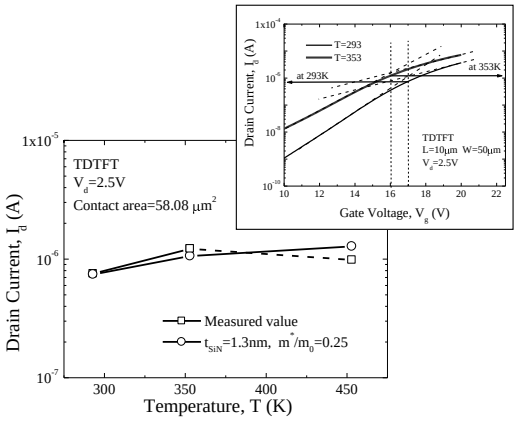

Fig. 5: Relationships between calculated and measured drain currents of TDTFT for conditions.

In the temperature range from 293 K to 353 K, it has been clarified that the dominant conduction mechanism of the TDTFT is the DT of SiN_X film. Here, the decrease of the drain current at the gate voltage application larger than the threshold gate voltage due to an insert of the tunneling dielectric film can be improved by formation of the tunneling dielectric film only to the drain side. Because, the gate voltage is applied to only the active layer, not distributed to the active layer and the tunneling dielectric film at the source side. Therefore, the ratio of the drain current at the gate voltage larger than the threshold gate voltage and that at the off-state voltage for the TDTFT increases in comparison with the conventional TFT.

IV. SUMMARY

We fabricated TDTFT that has a 1.7 nm-thick SiN_X films at the interface between the Al layer and n^+ doping layer. We measured the I_d-V_g characteristic from 293 to 623 K and discussed the conduction mechanism in the high temperatures. The simulation of the DT via SiN_X film was pursuit by dividing the electron distribution which contributes to the DT to the two areas. The DT from the both areas larger than the Fermi-energy affected by the temperature and smaller than the Fermi-energy non-affected by the temperature was considered.

As the result, when the thickness of SiN_X film and effective mass are 1.3 nm and 0.25, respectively, the relationship between the drain current and temperature reproduced the experimental results very closely. These results strongly indicate that the dominant conduction mechanism of the TDTFT in the higher temperatures is the DT. In addition, the tail area larger than the Fermi energy of Al greatly influences on the DT. The reason why the electron effective mass of 0.25 is used for the present simulation is that the effective mass decreases corresponding to the one-band model for the thin dielectric film.

References

[1] T. Uchida, "Recent Trends and Future Prospects of AM-LCDs", AM-LCD 99 Dig. Technical Papers, 1-4, (1999).

[2] K. Teruo, S. Yoshikazu, M. Kenji and S. Joji, "Development of Full Color Organic EL Display", IEICE technical report, **98**, 1-6, (1999).

[3] K. M. Chang, Y. H. Chung and G. M. Lin, "Anomalous Variations of OFF-State Leakage Current in Poly-Si TFT Under Static Stress", IEEE Electron Device Letter, **23**, .255-257 (2002).

[4] H. Hamada, H. Abe and Y. Miyai, "Development of High-Performance Poly-Si TFTs and Improvement of Image Characteristics for High-Definition LCD Light-Valves", The IEICE Trans. on Electronics (Japanese Edition), **.J84-C**, 65-75, (2001).

[5] N. Matsuo, H. Kihara, A. Yamamoto, N. Kawamoto and H. Hamada, "Proposal and Examination of New Type of TFT with Tunneling Dielectric Film at Both Ends of Channel Fabrication Area", The IEICE Trans. on electronics (Japanese Edition), C, **86**, 1070-1078 (2003).

[6] N. Matsuo, N. Kawamoto, A. Yamamoto and A. Heya, "Application of Tunneling Dielectric TFT on Double SOI to AM-OLED Drive Circuit", The IEICE Trans. on electronics (Japanese Edition), C, **89**, 409-415 (2006).

[7] N. Matsuo, T. Miura, H. Hamada and T. Miyoshi, "Application of Tunneling Effect for Thin Dielectric Film to MOS Transistor," The IEICE Trans. on Electronics (Japanese Edition), C, **J81-C**, .266-267 (1998).

[8] N. Matsuo, A. Fukushima, K. Ohkura, A. Heya and S. Yokoyama, "Fabrication of Tunneling Dielectric Thin-Film Transistor with Very Thin SiN_X Films onto Source and Drain", IEICE Electronics Express, **l.4**, 442-447 (2007).

[9] T. Kobayashi, N. Matsuto, T. Tochio, K. Ohkura, Y. Omura, S. Yokoyama and A. Heya, "Temperature Dependence of Drain Currents of Thin-Film Transistor with Very Thin SiN_X Film Formed at Source and Drain Reagion", The IEICE Trans. on electronics (Japanese Edition), C, **94**, 79 (2011).

[10] K.Boucart and A.M. Ionescu, "Double-Gate Tunnel FET With High-k Gate Dielectric," IEEE Trans. on Electron Devices, **54**, 1725-1733 (2007).

[11] E. H. Toh, G. H. Wang, L. Chan, D. Sylvester, C. H. Heng, G. S. Samudra and Y. C. Yeo,"Device Design and Scalability of a Double-Gate Tunneling Field-Effect Transistor with Silicon-Germanium Source," Jpn. J. Appl. Phys. **47**, 2593-2597 (2008).

[12] S. Toriyama, "Schottky-Barrier Metal–Oxide–Semiconductor Field-Effect Transistors as Resonant Tunneling Devices", Jpn. J. Appl. Phys. **49**, 104204-1 - 104204-4 (2010).

[13] A. Mallik and A. Chattopadhyay, "Observation of Current Enhancement Due to Drain-Induced Drain Tunneling in Tunnel Field-Effect Transistors", Jpn. J. Appl. Phys. **51**, 084301-1-084301-4 (2012).

[14] A.Mallik and A.Chattopadhyay, "Observation of Current Enhancement Due to Drain-Induced Tunneling in Tunnel Field-Effect Transistors", Jpn. J. Appl. Phys. .**51**, 084301-1-4 (2012).

[15] D. B. Duke, "Theory of Metal-Barrier-Metal Tunneling", Tunneling Phenomena in Solids, Chapter **4**, pp.31-46, (1969).

[16] W. A. Harrison, "Tunneling from an Independent-Particle Point of View" The Phys. Rev. **123**, 85 (1961)

[17] J. G. Simmons, F. L. Hsueh, and L. Faraone "Two-carrier conduction in MOS tunnel-oxides II-theory." Solid-State Electronics, **27**, 1131-1139 (1984).

[18] N. Matsuo, Y. Takami and H. Kihara, "Analysis of direct tunneling for thin SiO_2 film by Wentzel, Kramers, Brillouin method-considering tail of distribution function", Solid-State Electronics, **47**, 161-163 (2003).

[19] A. S. Grove, "Physics and Technology of Semiconductor Devices" John Wiley and Sons, Inc., New York, London, Sydney 12 , pp. 104, (1967).

[20] H. Kondo, S. Zaima, M. Hori, A. Sakai and M. Ogawa, "Initial Stage of Processes and Energy Bandgap Formation in Nitridation of Silicon Surface Using Nitrogen Radicals" J. Vac. Soc. Jpn., **50**, 665-671 (2007).

[21] N. Matsuo, J. Yamauchi, Y. Kitagwa and T. Miyoshi, "Analysis of Effective Mass of Tunneling Electron through Thin SiO_2 Film by WKB Method" The IEICE Trans. on Electronics (Japanese Edition), C, **83**, 577-580 (2000).
[22] B. Brar, G. D. Wilk, and A. C. Seabaugh, "Direct extraction of the electron tunneling effective mass in ultrathin SiO_2", Appl. Phys. Lett. **69**, 2728-2730 (1996).
[23] E. O. Kane and E. I. Blount, chapter 6, "Intarband Tunnleing." pp. 79-91, in "Tunneling Phenomena in Solids." Edited by E. Burstein and S. Lundqvist, PLENUM PRESS, New York, (1969).
[24] M. Hiroshima, T. Yasdaka, S. Miyazaki and M. Hirose, "Electron Tunnleing through Ultrathin Gate Oxide Formed on Hydrogen-Terminated Si(100) Surfaces", Jpn. J. Appl. Phys. **33**, No. 295-398 (1994).